AIP | The Journal of Chemical Physics

Phases and amplitudes of recurrences in autocorrelation function by a simple classical trajectory method

Petra Žďánská and Nimrod Moiseyev

Citation: The Journal of Chemical Physics **115**, 10608 (2001); doi: 10.1063/1.1416873
View online: http://dx.doi.org/10.1063/1.1416873
View Table of Contents: http://scitation.aip.org/content/aip/journal/jcp/115/23?ver=pdfcov
Published by the AIP Publishing

Phases and amplitudes of recurrences in autocorrelation function by a simple classical trajectory method

Petra Žďánská and Nimrod Moiseyev[a)]
Department of Chemistry and Minerva Center of Nonlinear Physics in Complex Systems, Technion—Israel Institute of Technology, Haifa 32000, Israel

(Received 9 August 2001; accepted 19 September 2001)

The interference between time-dependent recurrences in the quantum autocorrelation function is eliminated by carrying out orthogonal transformations in the time-energy domain. The time-dependent phases and amplitudes of the individual recurrences are compared with the results obtained from simple classical trajectory calculations. Using classical trajectories we calculate a two-dimensional survival probability which is defined in the time and energy domain. The two-dimensional survival probability provides the phase and enables to distinguish between overlapping recurrences. Remarkable agreement between the quantum and classical results is obtained for the initial Gaussian wave packet which is preferentially located either in the regular or in the chaotic regimes in the classical phase space of the Pullen–Edmonds Hamiltonian (nonlinearly coupled two harmonic oscillators). A novel method which enables to determine the molecular potential energy surfaces from a measured absorption or emission spectra is proposed. The method employs the matching of Wigner transforms of individual quantum recurrences with the two-dimensional classical survival probability. © *2001 American Institute of Physics.*
[DOI: 10.1063/1.1416873]

I. INTRODUCTION

Many chemical systems can be studied by means of semiclassical methods due to the heavy masses of the nuclei. Semiclassical calculations aim to evaluate a time-dependent wave function using the Van Vleck–Gutzwiller propagator,[1] instead of the quantum evolution operator. The direct numerical evaluation of the Van Vleck–Gutzwiller propagator is numerically hardly feasible even for one-dimensional systems, as it is defined as a double boundary problem and it encounters singularities along the integration path. Numerically, more tractable approaches are the initial value representation[2] and the integral expressions for the semiclassical time-dependent propagator, namely the Herman–Kluk formalism using the frozen Gaussian method.[3–5] Both approaches are equivalent to the rigorous semiclassical propagation. They have been applied to study the dynamics of model and real, regular and mixed chaotic systems.[6–10] Recently, the quasienergy spectrum of a periodically driven quantum system has been constructed from classical dynamics by means of the semiclassical initial value representation using coherent states.[11] For very large mixed regular and chaotic systems these calculations, however, can become complicated and require a substantial numerical effort.

Simplifying approaches to the semiclassical propagation are developed that are applicable even for very large systems.[12,13] Among them, two methods are exceptionally simple and general, both of them are linear approximations to the rigorous semiclassical dynamics: The frozen Gaussian approximation (FGA)[14] and the Wigner phase space method.[15] Their transparent behavior and low-computational costs make them good candidates for the study of very large systems. FGA builds up the wave function using one single classical trajectory which is developed in time. The wave function remains in a form of Gaussian for the entire time of the propagation. The method is very fast, it provides the many-dimensional wave function, but it is accurate only for a short time of the propagation. Often, this period of time is not long enough to evaluate vibrationally resolved spectra for systems of a chemical interest. The reason is that for anharmonic and mixed chaotic systems the time-dependent wave function distorts from a Gaussian shape very quickly. Namely, it bifurcates and develops a nodal structure. The second approach mentioned above is the Wigner phase space method. Within the framework of this approach, the initial wave function is mapped onto the classical phase space using the Wigner transform.[16] By giving each trajectory its initial *quantum* weight according to the Wigner distribution of the initial wave packet, one obtains a phase-space representation of the quantum time-dependent wave function. By Monte Carlo integration over the phase space one is able to obtain time-dependent amplitudes of quantum expectation values. The Wigner phase space method uses only classical trajectory propagation. Therefore, it does not suffer from the evaluation of highly oscillatory phase integrals which is encountered in a precise semiclassical approach. The correct treatment of bifurcations of the wave function is intermediated by propagating of many classical trajectories which trace the whole phase space reached by the wave function. The disadvantage of the Wigner phase space method is that it does not provide the quantum phases of the expectation values. It should be also mentioned here that despite of the fact that the trajectories trace correctly the phase space occupied

a)Electronic mail: nimrod@chemistry.technion.ac.il

by the semiclassical wave function, the method does not provide satisfactory results when the propagation time is long.

Our work is motivated by the desire of developing a computational algorithm which enables one to study the dynamics of very large systems for a very long time of propagation. It seems to us that in order to be able to study the dynamics of large systems we should not insist on the use of fully semiclassical methods but rather try to base the numerical efforts on the use of simple classical trajectory calculations. The question is how far we can go in this kind of approach. Here we address ourselves to the following question. Can we calculate the amplitude and the phase of the quantum autocorrelation functions by the use of classical trajectory calculations for sufficiently long time that enables the calculation of the spectrum and other properties of the studied system? A long time ago, Heller[15] showed that the amplitude of the autocorrelation function can be calculated by carrying out classical trajectory calculations up to the time when the quantum interference completely destroys the typical recurrence behavior of the autocorrelation functions. He termed his approach the ''Wigner phase space method'' (we mention it above). Recently, Garashchuk and Tannor[17] have introduced a way to calculate the phase of the autocorrelation function upon this approach. However, it appears that within their approach enormous number of trajectories are needed to reach convergence. Sun, Wang, and Miller[18] have derived the Wigner phase space method by means of the linearized semiclassical initial value representation.

Our paper is organized as follows. In Sec. II we propose a method that enables expanding the quantum autocorrelation function $C(t)$ in a series expansion of time-dependent terms, $C(t)=\Sigma_m C_m(t)$, such that each one of these terms is associated with a specific single recurrence. We show that the time-dependent recurrences $C_m(t)$ overlap in general cases. Therefore, the interference eliminates their fingerprints from the autocorrelation function $C(t)$. The Wigner transforms $Z_m(t,E)$ of the recurrences $C_m(t)$ are constructed. A positive definite partial survival probability is defined as $Z^{\mathrm{mod}}(t,E)=\Sigma_m Z_m(t,E)$.

In Sec. III we represent the classical analog of the function $Z^{\mathrm{mod}}(t,E)$, denoted by $S(t,E)$. $S(t,E)$ is obtained from the calculation of the partial overlap between the Wigner distribution of the initial wave packet and the time-dependent phase space distribution which is represented by the positions and momenta of classical trajectories with the classical energy E.

In Sec. IV we provide the classical approximation to complex recurrences in the autocorrelation function, $C_m^S(t)$. The recurrences $C_m^S(t)$ are calculated up to their time-independent phase factors only from the classical modified survival probability $S(t,E)$. In order to show the accuracy of the present calculation, we insert the time-independent phase factors obtained from the quantum recurrences $C_m(t)$ into the evaluation of the classical complex autocorrelation function. A remarkable agreement between the classical complex autocorrelation function and the quantum one has been obtained. We evaluate the amplitude of the autocorrelation function also by the method of Heller.[15] The new and Heller's methods provide the same amplitudes up to the point where the functions $C_m^S(t)$ start to overlap. In the region where the recurrences overlap, the accuracy of Heller's method suddenly decays, whereas, our method provides accurate results for a very long time of propagation.

The proposed method is illustrated numerically for a two-dimensional model Hamiltonian which consists of two nonlinearly coupled harmonic oscillators. This Hamiltonian, known as the Pullen–Edmonds Hamiltonian,[19] has been used before for testing new theories and computational algorithms which were developed in the studies of quantum chaos in nonlinear systems (see, for example, Refs. 20 and 21 and references therein). The Pullen–Edmonds Hamiltonian is a mixed chaotic/regular classical system. The Poincaré surface of section of the Pullen–Edmonds Hamiltonian at $E=21$ a.u. is shown in Fig. 1. Two different Gaussian wave packets have served as initial states in our calculations: In Fig. 1(a) the center of the initial Gaussian wave packet is located in the regular region of the phase space while in Fig. 1(b) the center of the initial wave packet is located in the chaotic region of the phase space. The quantum Hamiltonian has a discrete spectrum and supports bound states only.

In Sec. V we propose a practical application of the present method. This method enables one to determine the molecular potential energy surface from a measured absorption–emission spectra. Our method is based on the assumption that the recurrences $C_m(t)$ are sensitive to the potential parameters. If the quantum autocorrelation function is known one can find the potential energy surface by optimizing the potential parameters to minimize the two-dimensional (2D) function, $\int \mathrm{d}t\mathrm{d}E[S(t,E)-Z^{\mathrm{mod}}(t,E)]^2$. The method gives unique results for our numerically studied case. The use of this method for the determination of the ground or excited potential energy surfaces of polyatomic molecules from a given autocorrelation function by carrying out classical trajectory calculations only, are under current studies. It should be stressed, however, that we do not provide a method for solving the inverse problem for most general cases but one can use our method to optimize limited number of potential parameters.

In the Appendix we prove that our method to obtain the amplitude and the phase of the autocorrelation function is a linearized approach to the rigorous semiclassical propagation. Our proof is inspired by the work of Sun, Wang, and Miller.[18] We attempt to complement their study by taking into consideration the Maslov indices associated with different recurrences. We show that the short-time applicability of the Wigner phase space method results from neglecting of the interference effects between trajectories with different Maslov indices.

II. MODIFIED QUANTUM AUTOCORRELATION FUNCTION

This section is devoted to the analysis of the quantum autocorrelation function defined by the equation

$$C(t)=\int \mathrm{d}\boldsymbol{q}\Psi^*(\boldsymbol{q})e^{-i\hat{H}t/\hbar}\Psi(\boldsymbol{q}), \tag{1}$$

where $\Psi(\boldsymbol{q})$ is the initial wave function. We illustrate our discussion on a concrete example. In Figs. 2(a) and 2(b) we

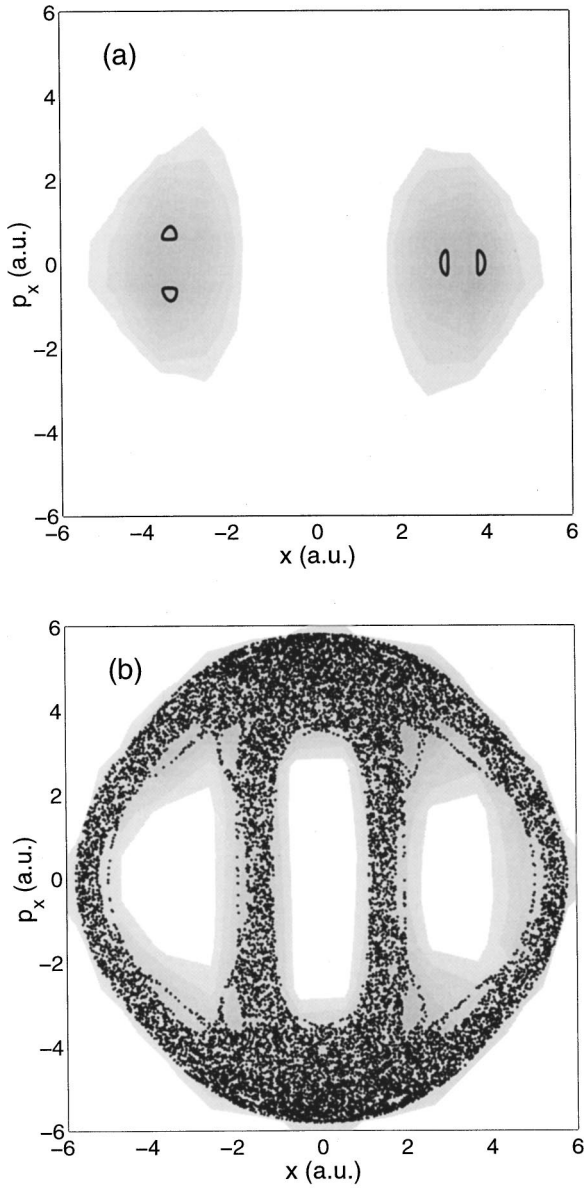

FIG. 1. Poincaré surfaces of section obtained for the Pullen–Edmonds model Hamiltonian for $p_y=0$. The dots represent the central trajectories of the initial Gaussian wave packets for the time period 8×10^5 a.u., while the shadow regions represent the phase space occupied by the propagating classical wave packet for the time period 40 a.u. (a) The central trajectory is localized in the regular anharmonic region of the classical phase space. (b) The central trajectory is localized in the chaotic region of the classical phase space. The classical wave packet covers in a relatively short time period of 40 a.u. the chaotic region.

present the real parts and amplitudes of autocorrelation functions, $C(t)$, which were obtained for a model Hamiltonian of nonlinearly coupled two harmonic oscillators

$$V(q_1,q_2)=\frac{q_1^2}{2}+\frac{q_2^2}{2}+\lambda q_1^2 q_2^2, \tag{2}$$

where $\lambda=0.05$ a.u. This model which is known as the Pullen–Edmonds Hamiltonian has been widely used as a model for testing new theories and interpretations of quantum chaos. We studied two cases. In the first case the center $(\boldsymbol{q}_0,\boldsymbol{p}_0)$ of the initial the Gaussian wave packet

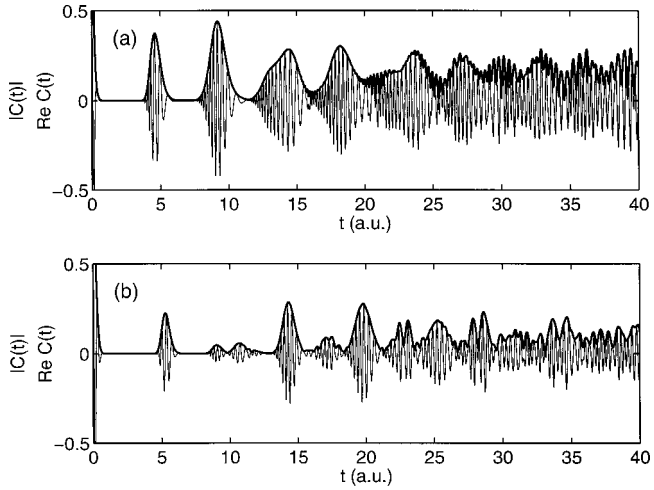

FIG. 2. The autocorrelation functions, $C(t)$, obtained from quantum-mechanical calculations. The center of the initial Gaussian wave packet is located: (a) in the regular region of the classical phase space; (b) in the chaotic region of the classical phase space. The thick line stands for $|C(t)|$ while the thin line represents Re $C(t)$.

$$\Psi(\boldsymbol{q})=\frac{1}{\sqrt{\pi}}\exp\left[\frac{(\boldsymbol{q}-\boldsymbol{q}_0)^2}{2}+i\frac{\boldsymbol{q}\boldsymbol{p}_0}{\hbar}\right], \tag{3}$$

is localized in the regular region of the classical phase space, where $\boldsymbol{q}_0=[4\text{ a.u.}, 2.957\text{ a.u.}]$, $\boldsymbol{p}_0=[0\text{ a.u.}, 0\text{ a.u.}]$. In the second case the center of the initial Gaussian wave packet is localized in the chaotic region, where $\boldsymbol{q}_0=[4\text{ a.u.}, 1.645\text{ a.u.}]$, $\boldsymbol{p}_0=[0\text{ a.u.}, 4\text{ a.u.}]$. The expectation value of energy for the both studied cases is 21 a.u. One can see from the results presented in Figs. 2(a) and 2(b) that for a short period of time, $t\leqslant 20$ a.u., the recurrences are well defined and are separated from one another. However, as time passes the recurrences disappear due to quantum interference effects. Let us assume that a recurrence m which is not distinguishable in t-representation can be determined from the autocorrelation function in a t'-representation, where it is well isolated from the other recurrences. The autocorrelation function in the t'-representation is obtained by the following transformation:

$$C'(t';\alpha)=\int_{-\infty}^{+\infty}F(t,t';\alpha)C(t)\mathrm{d}t, \tag{4}$$

where

$$F(t,t';\alpha)\sim\exp\left[\frac{i}{\hbar}\left(-\frac{tt'}{\sin\alpha}+\frac{t^2+t'^2}{2\tan\alpha}\right)\right],$$

$$\text{for } 0<\alpha\leqslant\frac{\pi}{2}, \tag{5}$$

and

$$F(t,t';\alpha)=\delta(t-t'), \quad \text{for } \alpha=0. \tag{6}$$

The constant prefactor of the transformation function $F(t,t';\alpha)$ defined in Eq. (5) varies according to the integration region of the transformation. The function $F(t,t';\alpha)$ is the complex conjugate of an eigenfunction of $\hat{t}$ in

t'-representation and an eigenfunction of $\hat{t}'$ in t-representation. $\hat{t}$ and $\hat{t}'$ are related by the orthogonal transformation

$$\begin{bmatrix} \hat{t}' \\ \hat{E}' \end{bmatrix} = \mathbf{T}(\alpha) \begin{bmatrix} \hat{t} \\ \hat{E} \end{bmatrix}, \tag{7}$$

where,

$$\mathbf{T}(\alpha) = \begin{bmatrix} \cos\alpha & \sin\alpha \\ -\sin\alpha & \cos\alpha \end{bmatrix}. \tag{8}$$

The energy operator is defined as

$$\hat{E} = -i\hbar \frac{\mathrm{d}}{\mathrm{d}t}. \tag{9}$$

As usual, the commutation relations imply that

$$[\hat{t},\hat{E}] = i\hbar, \quad [\hat{t}',\hat{E}'] = i\hbar. \tag{10}$$

The parameter α is adjusted to eliminate the quantum interference between the mth recurrence and its adjacent neighbors. For illustration reasons we discuss the transformations of autocorrelation functions $C'(t';\alpha)$ obtained for specific values of the angle α. The transformation $F(t,t';\pi/15)$ is performed for the case when the wave packet undergoes mostly a regular motion [Fig. 3(a)]. The transformation enables us to distinguish between eight dominant recurrences starting from the initial decay peak, whereas only three separate recurrences are present in the original $C(t)$ [Fig. 2(a)]. Note, that each one of the dominant recurrences appends also low amplitude recurrences which cannot be separated by the present transformation. For the case of chaotic dynamics we carry out the transformation $F(t,t';\pi/30)$ [Fig. 3(b)]. About ten separated recurrences are obtained. Unlike the situation in the regular regime, the separated peeks do not show any fine structure. The transformations presented in Figs. 3(a) and 3(b) result in the separation of recurrences which are indistinguishable in the original autocorrelation function. The optimization of the angle α enables one to get a maximal separation between the different recurrences. The angle which is optimized to get a maximum separation of the mth recurrence from the others is denoted by α_m.

The mth recurrence is defined in the t'-representation in the interval $\langle t_m'^0, t_m'^f \rangle$. We perform the following back transform to the t-representation, which is a *finite* integral:

$$C_m(t) = \int_{t_m'^0}^{t_m'^f} F(t,t';-\alpha_m) C'(t';\alpha_m)\,\mathrm{d}t'. \tag{11}$$

The recurrence components $C_m(t)$ create a progression as shown in Figs. 4(a) and 4(b) for the two cases when the calculation is performed either in the regular or in the chaotic regimes, respectively. A comparison between the results presented in Figs. 2(a) and 2(b) and Figs. 4(a) and 4(b) clearly illustrates the recovery of the smooth recurrences from the quantum autocorrelation functions. Under the assumption that the recurrences are separable in the mixed time-energy representation, the original autocorrelation function is equal to the sum over all recurrences which can be isolated by our procedure

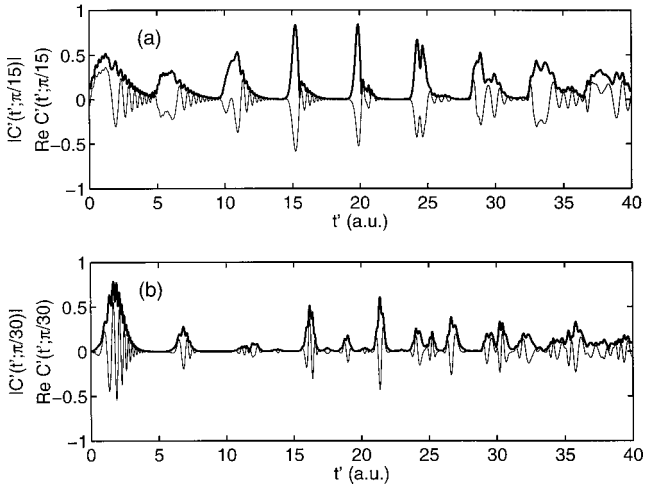

FIG. 3. The transformed autocorrelation functions $C'(t')$. The transformation in the mixed time-energy coordinate t' enables to resolve recurrences which overlap in the time domain. (a) The center of the initial Gaussian wave function is localized in the regular region of the classical phase space. The parameter of the transformation is $\alpha=\pi/15$. (b) The center of the initial Gaussian wave function is localized in the chaotic region of the classical phase space. The parameter of the transformation $\alpha=\pi/30$. The thick line stands for $|C'(t')|$ while the thin line represents Re $C'(t')$.

$$C(t) = \sum_{m=0}^{\infty} C_m(t). \tag{12}$$

The progression of recurrences $C_m(t)$ [Figs. 4(a) and 4(b)] begins with a few nonoverlapping ones. At later times of propagation the recurrences overlap. The sum of those recurrences which overlap results in a strong interference and the typical recurrence pattern in autocorrelation function is destroyed. It should be stressed here that the overall time-independent phase factors of the individual recurrences are crucial for the evaluation of the autocorrelation function. The forth and back transformations described below preserve them correctly.

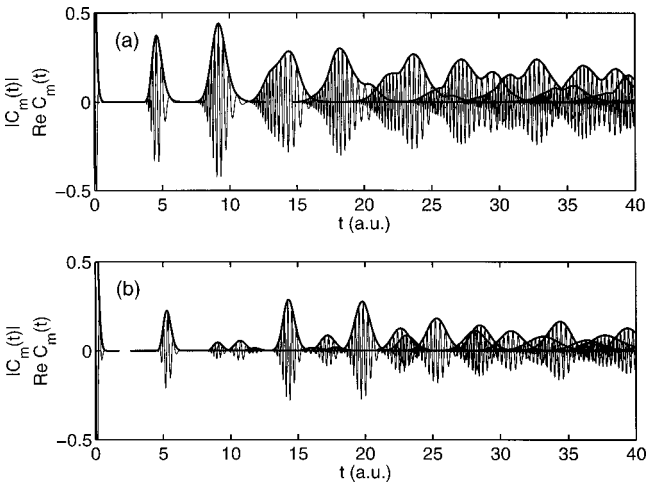

FIG. 4. The recurrences in the quantum autocorrelation functions isolated by forward and backward transformations performed in the time-energy domain. The center of the initial Gaussian wave function is localized: (a) in the regular region of the classical phase space; (b) in the chaotic region.

The recurrences are separable in the mixed time-energy representation [Eqs. (7) and (8)]. This fact is an indication that each one of the recurrences occupies a different region in the two-dimensional time-energy "phase space." The projection of the time-dependent complex autocorrelation function $C(t)$ and recurrences $C_m(t)$ into the two-dimensional time-energy domain is intermediated by the Wigner transform. The Wigner transform of functions and operators represents an alternative tool to the exact formulation of quantum mechanics.[16] It has been widely used for rendering wave functions and time-dependent signals in a phase space of conjugate variables. The physical meaning of the Wigner transform $Z(t,E)$ of the autocorrelation function is the survival quasi-probability at the energy "shell" E. The definition of the function $Z(t,E)$ is as follows:

$$Z(t,E)=\frac{1}{2\pi\hbar}\int_{-\infty}^{+\infty}A(t,\tau)e^{-iE\tau/\hbar}\mathrm{d}\tau, \tag{13}$$

where A is related to the density matrix by the equation

$$A(t,\tau)=C^*\left(t+\frac{\tau}{2}\right)C\left(t-\frac{\tau}{2}\right). \tag{14}$$

The transform of the function $Z(t,E)$ back to $C(t)$ is possible, up to a time-independent phase factor, which is lost in Eq. (14). It follows from the Eq. (13) that the density matrix is the Fourier transform of the Wigner distribution

$$A(t,\tau)=\int_{-\infty}^{+\infty}\mathrm{d}EZ(t,E)e^{iE\tau/\hbar}. \tag{15}$$

The derivatives $[\partial^n A(t,\tau)/\partial\tau^n]_{\tau=0}$ can be evaluated from Eqs. (14) and (15). A comparison between the two type of calculations provides

$$\left[\frac{\partial^n C^*(t+\tau/2)C(t-\tau/2)}{\partial\tau^n}\right]_{\tau=0}=\left(\frac{i}{\hbar}\right)^n Z^{(n)}(t), \tag{16}$$

where the "hydrodynamical moments" $Z^{(n)}(t)$ of the Wigner distribution are defined as,

$$Z^{(n)}(t)=\int_{-\infty}^{+\infty}E^nZ(t,E)\mathrm{d}E. \tag{17}$$

For $n=0$ we obtain the survival probability as the zero-order "hydrodynamical moment" of $Z(t,E)$

$$|C(t)|^2=\int_{-\infty}^{+\infty}Z(t,E)\mathrm{d}E. \tag{18}$$

For $n=1$ we obtain an expression for the phase of the autocorrelation function, $C(t)=|C(t)|\exp[i/\hbar\phi(t)]$

$$\frac{\mathrm{d}\phi}{\mathrm{d}t}=-\frac{\int_{-\infty}^{+\infty}EZ(t,E)\mathrm{d}E}{\int_{-\infty}^{+\infty}Z(t,E)\mathrm{d}E}. \tag{19}$$

Therefore,

$$C(t)=e^{iK}\sqrt{Z^{(0)}(t)}\exp\left[\frac{i}{\hbar}\int^t\frac{Z^{(1)}(t')}{Z^{(0)}(t')}\mathrm{d}t'\right], \tag{20}$$

where K is a time-independent phase factor. In general, the Wigner transform does not provide a positive definite function. The Wigner transform of the autocorrelation function $Z(t,E)$ is a highly oscillatory function for any periodic system.[22] On the other hand, the amplitude and the phase of recurrences $C_m(t)$ are smooth time-dependent functions which acquire positive definite Wigner transforms, $Z_m(t,E)$, defined by the equation:

$$Z_m(t,E)=\frac{1}{2\pi\hbar}\int_{-\infty}^{+\infty}C_m^*\left(t+\frac{\tau}{2}\right)C_m\left(t-\frac{\tau}{2}\right)e^{-iE\tau/\hbar}\mathrm{d}\tau. \tag{21}$$

Using the definition of $Z_m(t,E)$ we can write the function $Z(t,E)$ as a sum of the "auto-terms" $Z_m(t,E)$ and oscillatory "cross-terms" $Z_{m,m'}$, which are defined by,

$$Z_{m,m'}(t,E)=\frac{1}{2\pi\hbar}\int_{-\infty}^{+\infty}C_m^*\left(t+\frac{\tau}{2}\right)\times C_{m'}\left(t-\frac{\tau}{2}\right)e^{-iE\tau/\hbar}\mathrm{d}\tau. \tag{22}$$

The auto-terms carry the information about the autocorrelation function up to time-independent phase factors of the recurrences. The *cross-term deleted* Wigner transform of the autocorrelation function can be defined as a sum of the auto-terms[23]

$$Z^{\mathrm{mod}}(t,E)=\sum_m Z_m(t,E). \tag{23}$$

The positive definite function $Z^{\mathrm{mod}}(t,E)$ is associated with the survival probability for the energy shell E. We refer to it as "the partial survival probability" throughout our paper. In Figs. 5(a) and 5(b) we represent contour plots of $[-\log Z^{\mathrm{mod}}(t,E)]$. They are characterized by a sequence of isolated recurrences. The result presented in Fig. 5(a) is obtained for the case where the initial state is a Gaussian wave packet which is localized in the regular regime. For the case of regular motion we observe evidence for a single frequency *per* energy shell. A small portion of $Z^{\mathrm{mod}}(t,E)$ gets an oscillatory behavior which is a consequence of the imperfect separation of minor recurrences (see the discussion above). The partial survival probability which is presented in Fig. 5(b) is obtained for the case where the initial wave packet is located in the chaotic regime of the classical phase space. For the chaotic motion we observe a contribution of different frequencies to each one of the energy shells.

The Husimi transform of the autocorrelation function, which is another positive definite representation of the autocorrelation function in the time-energy domain, is defined by[16]

$$H(t,E)=\frac{1}{\sqrt{\pi}}\left|\int\mathrm{d}t'C^*(t)\exp\left[-\frac{(t'-t)^2}{2\sigma}+i\frac{t'E}{\hbar}\right]\right|^2. \tag{24}$$

The Husimi transform leads to a lower resolution in the time-energy domain than the proposed algorithm when we use the Wigner transforms of the individual recurrences. The Husimi transform of the autocorrelation function for the case where the initial wave packet is localized in the regular region of the classical phase space is represented in Fig. 6(a). The recurrences observed in Fig. 6(a) are significantly broadened

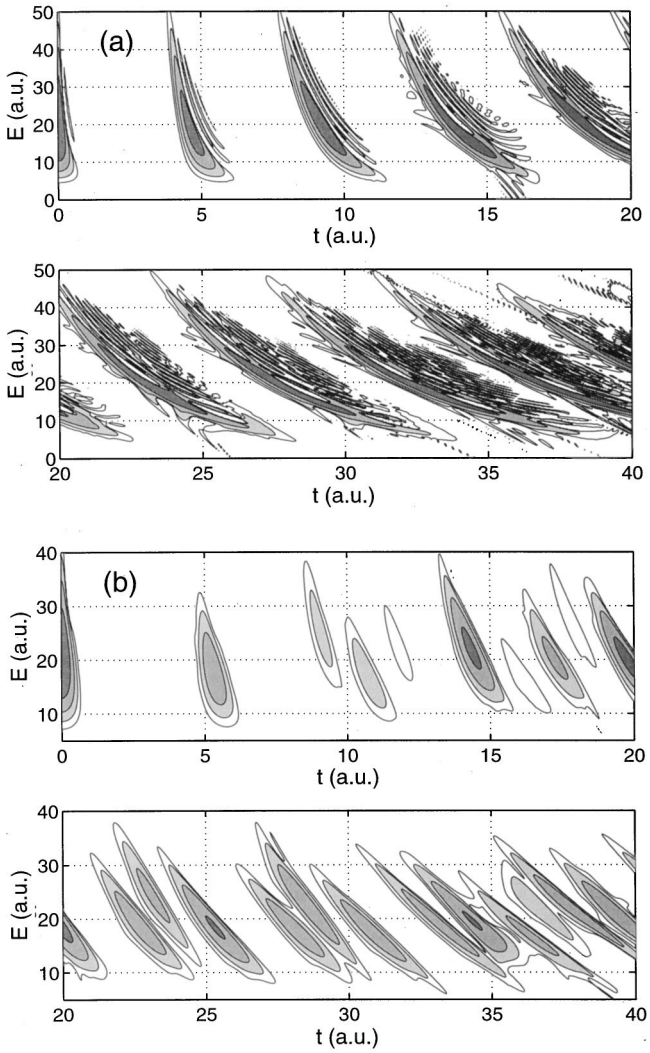

FIG. 5. The quantum partial survival probability $Z^{\mathrm{mod}}(t,E)$. The sequence of clearly isolated recurrences is obtained by carrying out the Wigner transforms of $C_m(t)$. The center of the initial Gaussian wave function is localized: (a) in the regular region of the classical phase space; (b) in the chaotic region.

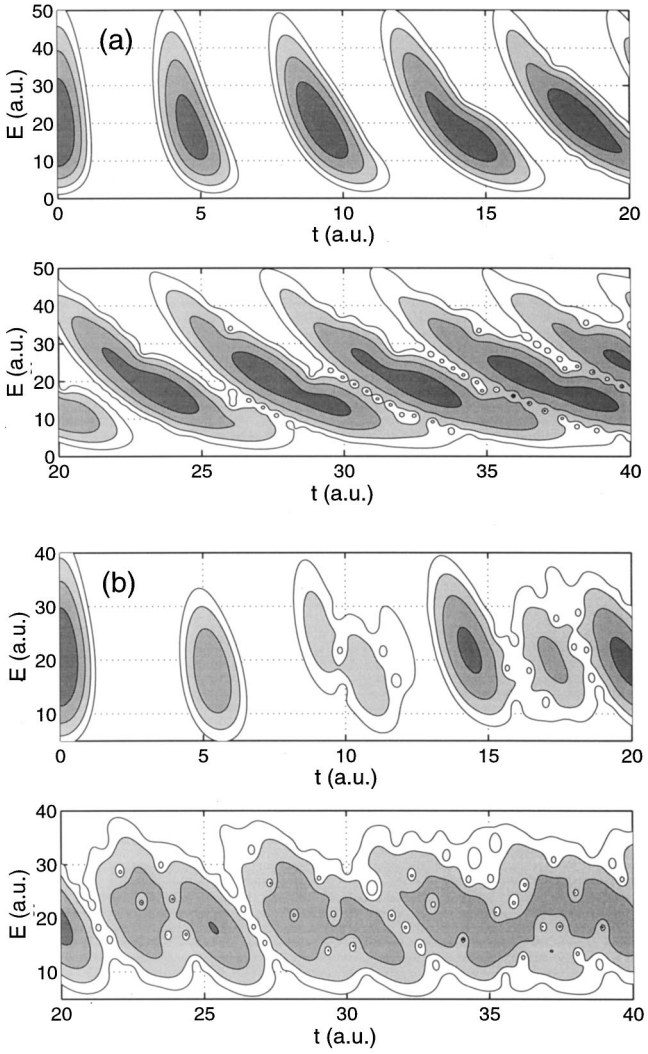

FIG. 6. The Husimi transforms of the quantum autocorrelation function. The center of the initial Gaussian wave function is localized: (a) in the regular region of the classical phase space; (b) in the chaotic region.

compared to the recurrences observed in Fig. 5(a). The Husimi transform of the autocorrelation function for the case where the initial wave packet is localized in the chaotic region of the classical phase space is represented in Fig. 6(b). Similarly as for the regular case, the recurrences obtained by the Husimi transform are broader than the widths of the recurrences obtained by the Wigner transform [Fig. 5(b)]. As one can see from the results presented in Fig. 6(b), the recurrence pattern is totally suppressed in Husimi representation of $C(t)$ the propagation time which is longer than 20 a.u. Note that on the other hand a clear recurrence pattern provided holds on the partial survival probability [Fig. 5(b)].

III. THE CLASSICAL ANALOG OF THE QUANTUM PARTIAL SURVIVAL PROBABILITY

The partial survival probability $Z^{\mathrm{mod}}(t,E)$ provides the survival probability for a specific energy shell E. Let us define a classical function $S(t,E)$ which has the same physical interpretation. In this section we give an intuitive approach and in the Appendix we give a rigorous proof. Let us start with the quantum definition of the survival probability using the Wigner distribution of the initial and the final wave packets

$$|C(t)|^2 = \int \mathrm{d}\boldsymbol{q}\mathrm{d}\boldsymbol{p} W(\boldsymbol{q},\boldsymbol{p}) W(\boldsymbol{q},\boldsymbol{p},t), \tag{25}$$

where $W(\boldsymbol{q},\boldsymbol{p})$ is the Wigner distribution of the initial wave packet $\Psi(\boldsymbol{q})$, defined as follows:

$$W(\boldsymbol{q},\boldsymbol{p}) = \frac{1}{(2\pi\hbar)^F} \int \mathrm{d}\Delta\boldsymbol{q} \Psi^*\left(\boldsymbol{q}+\frac{\Delta\boldsymbol{q}}{2}\right) \times \Psi\left(\boldsymbol{q}-\frac{\Delta\boldsymbol{q}}{2}\right) e^{i\boldsymbol{p}\Delta\boldsymbol{q}/\hbar}, \tag{26}$$

where F is the number of degrees of freedom of the multidimensional system. Similarly, $W(\boldsymbol{q},\boldsymbol{p},t)$ is the Wigner distribution of the quantum wave packet $\exp(-i\hat{H}t/\hbar)\Psi(\boldsymbol{q})$. Note that Eq. (25) is the exact quantum survival probability. Within the Wigner phase space method,[15] the quantum

Wigner function $W(\boldsymbol{q},\boldsymbol{p},t)$ is replaced by a classical time-dependent distribution function $W(\boldsymbol{q}_t,\boldsymbol{p}_t)$. The survival probability within this approximation is given by

$$|C^{\mathrm{WPS}}(t)|^2=\int \mathrm{d}\boldsymbol{q}_0\mathrm{d}\boldsymbol{p}_0 W(\boldsymbol{q}_0,\boldsymbol{p}_0)W(\boldsymbol{q}_t,\boldsymbol{p}_t), \tag{27}$$

where $\boldsymbol{q}_0$, $\boldsymbol{p}_0$ are initial positions and momenta of classical trajectories and $\boldsymbol{q}_t(\boldsymbol{q}_0,\boldsymbol{p}_0,t)$, $\boldsymbol{p}_t(\boldsymbol{q}_0,\boldsymbol{p}_0,t)$ are the corresponding classical positions and momenta at time t. In order to obtain the survival probability in both coordinates t and E, we integrate only over a subspace for which $H(\boldsymbol{q}_0,\boldsymbol{p}_0)=E$:

$$S(t,E)=\int' \mathrm{d}\boldsymbol{q}_0\mathrm{d}\boldsymbol{p}_0 W(\boldsymbol{q}_0,\boldsymbol{p}_0)W(\boldsymbol{q}_t,\boldsymbol{p}_t)\delta[H(\boldsymbol{q}_0,\boldsymbol{p}_0)-E], \tag{28}$$

where H is the classical Hamiltonian. Equation (28) represents the classical definition of the partial survival probability $Z^{\mathrm{mod}}(t,E)$.

When the Monte Carlo integration is used, the initial positions and momenta $\boldsymbol{q}_0^j$, $\boldsymbol{p}_0^j$, are preferentially distributed in the region of the phase space where the initial wave packet is localized. The algorithm of choosing the Monte Carlo points is described as follows: A random position in the phase space $\boldsymbol{q}_0^j$, $\boldsymbol{p}_0^j$ is generated; the value of the initial Wigner distribution $W(\boldsymbol{q}_0^j,\boldsymbol{p}_0^j)$ is compared with a random number $\aleph$ the random number $\aleph$ spans evenly the range of possible values of W; if $W(\boldsymbol{q}_0^j,\boldsymbol{p}_0^j)>\aleph$, the point $\boldsymbol{q}_0^j$, $\boldsymbol{p}_0^j$ is accepted. The function $S(t,E)$ is calculated on a two-dimensional grid. Let us denote the energy grid points by E_k. From the Monte Carlo points which are associated with the energies $E=H(\boldsymbol{q}_0^j,\boldsymbol{p}_0^j)$, we select only those for which $E_k-\Delta E\leqslant E\leqslant E_k+\Delta E$ where $\Delta E\ll|E_{k+1}-E_k|$. Following this procedure we generate ''families'' of classical trajectories. Each ''family'' is associated with different energy, E_k. The number of classical trajectories in each family is N_k. Let us denote the trajectories by two indexes, k and n. Where, k stands for kth ''family'' of the classical trajectories and n is an internal family index notation. The initial classical trajectories are denoted as, $q_0^{k,n}$, $p_0^{k,n}$. $S(t,E)$ is obtained by the Monte Carlo integration

$$S(t,E_k)=\sum_{n=1}^{N_k} W(\boldsymbol{q}_t^{k,n},\boldsymbol{p}_t^{k,n}). \tag{29}$$

The presented semiclassical method has been applied to the Pullen–Edmonds model Hamiltonian for the same two initial wave packets which are described in the previous section. 50 000 trajectories have been used to obtain converged results, when $|E_{k+1}-E_k|=1$ a.u. and $\Delta E=10^{-5}$ a.u. Contour plots of $[-\log S(t,E)]$ [Figs. 7(a) and 7(b)] can be directly compared with the contour plots of $Z^{\mathrm{mod}}(t,E)$ [see Figs. 5(a) and 5(b)]. The classical and quantum results are in a remarkable agreement. Well isolated recurrences are observed all the way to the end of the propagation. The recurrences can be interpreted as the trace of a quasiperiodic motion. In the case of regular regime, the equal spacing of recurrences indicates only one type of a quasiperiodic motion. In the case of chaotic regime, the recurrences are spaced out irregularly which is an evidence for various types of quasiperiodic motions.

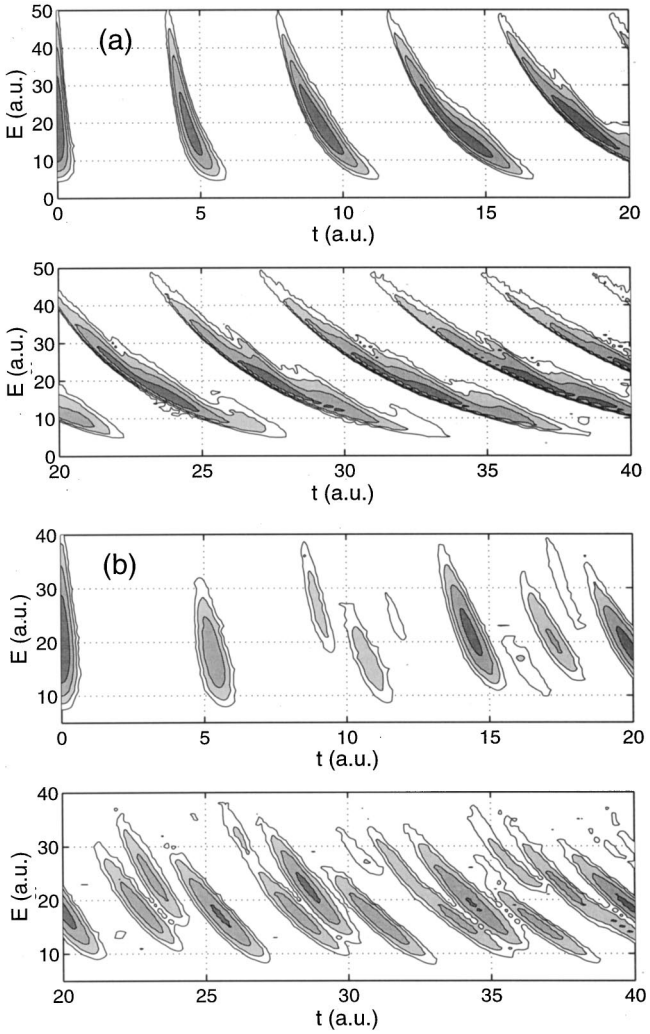

FIG. 7. The partial survival probability $S(t,E)$ obtained by classical trajectory propagations. The center of the initial Gaussian wave function is localized: (a) in the regular region of the classical phase space; (b) in the chaotic region.

IV. A COMPARISON BETWEEN AUTOCORRELATION FUNCTIONS OBTAINED FROM CLASSICAL AND QUANTUM CALCULATIONS

The fact that the classical function $S(t,E)$ is a very good approximation of the quantum partial survival probability $Z^{\mathrm{mod}}(t,E)$, indicates on the possibility to evaluate the complex recurrences $C_m(t)$ in the autocorrelation function from classical calculations. Unfortunately, the autocorrelation function cannot be obtained from our classical calculation since the time-independent phase factors of the recurrences are not included in the partial survival probability. The function $S(t,E)$ contains very well isolated recurrence components $S_m(t,E)$ (see Fig. 7). Each one of the functions $S_m(t,E)$ is transformed into the time-domain by using Eq. (20). The transformation provides the mth recurrence $C_m^S(t)$ up to the time-independent phase factor K_m

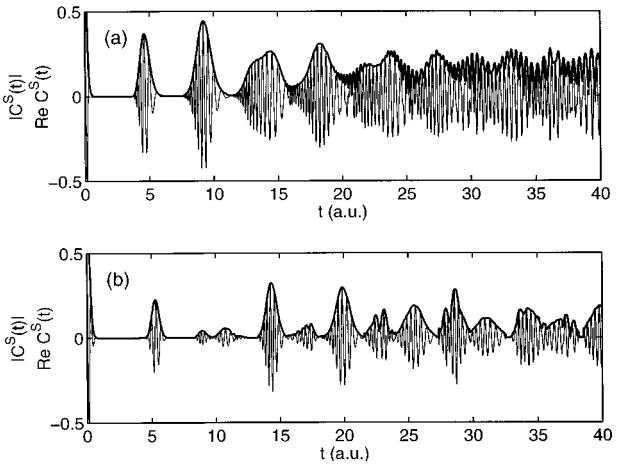

FIG. 8. The autocorrelation function calculated from classical trajectory calculations, $C^S(t)$, using the quantum time-independent phase factors. The center of the initial Gaussian wave function is localized: (a) in the regular region of the classical phase space; (b) in the chaotic region.

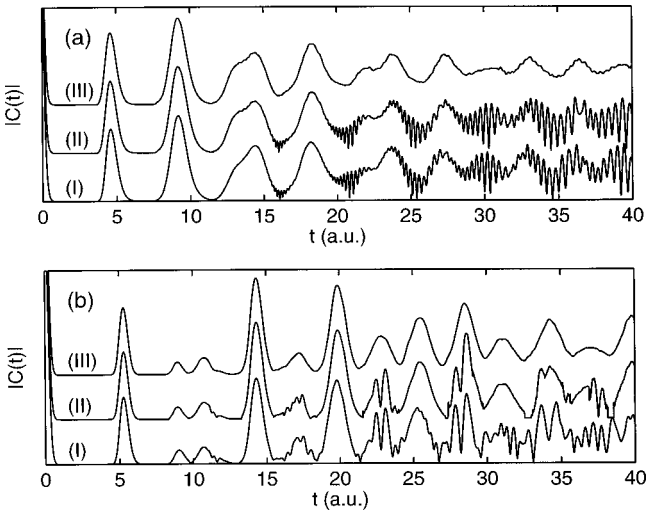

FIG. 9. The amplitude of the autocorrelation function obtained: (I) from the exact quantum calculations; (II) from the modified Wigner phase space method represented in our paper, using the quantum time-independent phase factors of the recurrences; (III) from the Wigner phase space method. The center of the initial Gaussian wave function is localized: (a) in the regular region of the classical phase space; (b) in the chaotic region.

$$C_m^S(t)=\sqrt{S_m^{(0)}(t)}\,\exp\left[\frac{i}{\hbar}\int^t \overline{E}_m(t')\mathrm{d}t'\right]. \tag{30}$$

$\overline{E}_m(t)$ stands for the averaged energy of those classical trajectories which contribute to the mth recurrence at time t. It is calculated by

$$\overline{E}_m(t)=\frac{S_m^{(1)}(t)}{S_m^{(0)}(t)}. \tag{31}$$

The ''hydrodynamical moments'' of the function $S_m(t,E)$ are defined as

$$S_m^{(n)}(t)=\int_{-\infty}^{+\infty} E^n S_m(t,E)\mathrm{d}E. \tag{32}$$

Borrowing the missing time-independent phase factors K_m from the quantum calculations we can evaluate the classical autocorrelation function $C^S(t)$. According to Eq. (12), the classical complex quantum autocorrelation function is given by

$$C^S(t)=\sum_m C_m^S e^{iK_m}. \tag{33}$$

In Figs. 8(a) and 8(b) we represent the results of $C^S(t)$ which were obtained for the Pullen–Edmonds model Hamiltonian. Figure 6(a) represents the result obtained when the classical dynamics starts from an initial Gaussian wave packet which is localized in the regular part of the phase space. In Fig. 6(b) we represent the result obtained when the initial wavepacket is localized in the chaotic region. In both cases the agreement between the classical and the quantum results is remarkable. Let us discuss two aspects of this calculation. The first one is the recovering of the time-dependent phase from the classical trajectory calculation. The second aspect is the contribution of interference between recurrences to the amplitude of the autocorrelation function.

For the calculation of the time-dependent phase, it is crucial to take into account the quantum interference between individual classical trajectories. Applying the rigorous semiclassical propagation, the phase is calculated for each one of the classical trajectories as the classical action along the classical path. Although the classical action $s(\boldsymbol{q}_0,\boldsymbol{p}_0,t)$ is a smooth function of the phase space variables, the imaginary exponential $\exp[is(\boldsymbol{q}_0,\boldsymbol{p}_0,t)/\hbar]$ is very oscillatory. The integration over the oscillatory exponential leads to a numerical convergence problem. In our approach, the interference between the trajectories is introduced by calculating of the averaged classical energy $\overline{E}_m(t)$ [Eqs. (30) and (31)]. The fact that the interference between trajectories is provided by the integration of energy, which a smooth function of the phase space variables and a constant of motion, considerably reduces the computational effort to evaluate the time-dependent phase.

The recurrences in the time-energy domain are associated with a quasi-periodic motion in the classical phase space. The sets of trajectories which form each one of the peaks in $S(t,E)$ are characterized by diverse classical paths through the phase space. Therefore, the overlap of recurrences in the time-domain is an indication for a ″long-range″ interference. Strictly speaking, and as shown in the Appendix, the long-range interference is the interference between trajectories which have visited a different number of caustic points on their paths. The long-range interference cannot be treated correctly within the Wigner phase space method. We calculate the classical survival probability which is obtained from the Wigner phase space method, as defined in Eq. (25). The results are compared with the exact quantum calculations and with the results obtained from our ''modified'' Wigner phase space method. The results are presented in Fig. 9(a) for the case of a regular motion and in Fig. 9(b) for the case of a chaotic motion. As one can see, the Wigner phase space method provides a very good result for a short period of time, until the interference between the recurrences takes an important role in the autocorrelation function.

A question may arise, for how long time of propagation

the new method is applicable. Does the approximation break down, for example, when seriously nonlinear effects set in? In Figs. 1(a) and 1(b) we demonstrate that the time-dependent wave function visits all regions of the mixed chaotic and regular phase space within a short propagation time of 40 a.u. This creates a significant difference between one trajectory when the time needed to visit the same phase space region is four orders of magnitude longer. This fact, together with the agreement between the quantum and the classical simulations reported below, give evidence that our method is able to capture the nonlinear effects. On the other hand it should be noted that as the time of propagation grows, the possibility to separate individual recurrences in the time-energy plane slowly decreases. The intuitive conclusion is that after a very long time of classical propagation, t_{lim}, the recurrences start to overlap in the time-energy plane. The time t_{lim} is associated with a measure of the chaotic behavior of multidimensional systems. For one-dimensional systems, $t_{\mathrm{lim}}\rightarrow\infty$ due to the conservation of the phase space volume.

V. POTENTIAL ENERGY SURFACES FROM CLASSICAL TRAJECTORY CALCULATIONS

The sensitivity of the calculated 2D function $S(t,E)$ to small variations of the potential parameters indicates on the possibility to determine the values of these parameters by matching the structures of $S(t,E)$ and $Z^{\mathrm{mod}}(t,E)$, where $Z^{\mathrm{mod}}(t,E)$ can be derived from a measured absorption or emission spectrum.[24] We use the Pullen–Edmonds model Hamiltonian to test this idea. We introduce two unknown potential parameters: The strength of the harmonic oscillator K and the nonlinear strength coupling parameter λ

$$V(q_1,q_2;K,\lambda)=\frac{K}{2}(q_1^2+q_2^2)+\lambda q_1^2 q_2^2. \tag{34}$$

In order to fit the parameters K and λ we search for the global minimum of the standard deviation $\sigma(K,\lambda)$

$$\sigma(K,\lambda)=\int \mathrm{d}E\,\mathrm{d}t[S(t,E;K,\lambda)-Z^{\mathrm{mod}}(t,E)]^2. \tag{35}$$

The function $S(t,E;K,\lambda)$ is calculated on a two-dimensional equidistant grid, $0<t<22.5$ a.u. and $8<E<43$ a.u. 2500 points for t and 8 points for E are used in our calculation. The initial wave function is a Gaussian wave packet which is localized in the chaotic region of the classical phase space as discussed in Sec. II. For the classical calculations only 500 trajectories are employed in order to obtain the function $S(t,E;K,\lambda)$. The global minimum of the surface of $\sigma(K,\lambda)$ is found using the random walk approach since the calculated values of $\sigma(K,\lambda)$ include a stochastic error. The algorithm which we used is as follows: (i) The initial guess of the potential parameters serves as the first position of the "random walker:" $K_{i=0}$, $\lambda_{i=0}$. (ii) $\sigma(K_i^j,\lambda_i^j)$ is evaluated at points which are randomly distributed in a small rectangle $(K_i-\Delta K)<K_i^j<(K_i+\Delta K)$, $(\lambda_i-\Delta\lambda)<\lambda_i^j<(\lambda_i+\Delta\lambda)$. (iii) The successive point of the random walker $K_{i+1}=K_i^j$, $\lambda_{i+1}=\lambda_i^j$ is chosen such that $\sigma(K_i^j,\lambda_i^j)<\sigma(K_i^{j-1},\lambda_i^{j-1})$. The effectiveness of the random walker is demonstrated on Fig. 10. The potential parameters are set initially far away from the expected minimum, $\lambda=0.2$, $K=2$. For the initial potential parameters the standard deviation between the classical and the reference quantum partial survival probability is $\sigma(2.0,0.2)>10$. The random walker is moved by steps of $\Delta\lambda=0.01$, $\Delta K=0.1$. The random walker spends about 150 classical evaluations before it finds a flat minimum characterized by the values of $\sigma<3$. This region is explored by the rest of total 3000 evaluated points. The values of $\sigma(K,\lambda)$ are used to obtain a smoothed incomplete surface which is displayed in Figs. 11(a) and 11(b). The global minimum is obtained for the expected potential parameters $K=1\pm0.1$, $\lambda=0.05\pm0.01$. A more precise determination of the potential parameters might be obtained by a secondary calculation starting close to the minimum found by the present calculation. To conclude, we demonstrate that from classical trajectory calculations one is able to find the correct potential parameters. We suggest this fitting procedure to find potential parameters of real systems in the regime of their semiclassical limit. A suitable problem is of a molecule which absorbs light in the visible or ultraviolet (UV) range and is electronically excited to an adiabatic potential energy surface.[24] From the vibrationally resolved absorption spectrum and from the knowledge of the initial vibrational state, we can calculate the quantum function $Z^{\mathrm{mod}}(t,E)$. If a reasonable functional form of the potential of the electronically excited state is available, its parameters can be optimized to fit the function $S(t,E)$ to the experimental data. The method may be sensitive to the precision of the initial wave packet and to the transition moments, too. This sensitivity is supposed to be rather negligible for the cases where the initial wave packet is a localized vibrational ground state. For other cases where the uncertainty in the knowledge of the initial wave packet and in the transition moments is expected to compete or even

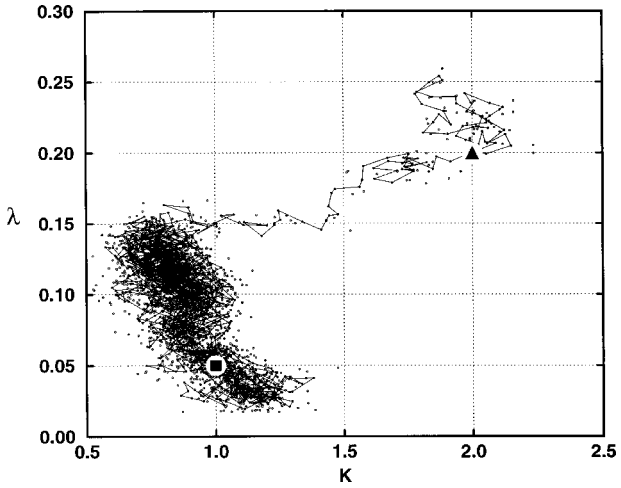

FIG. 10. The potential parameters K and λ of the Pullen–Edmonds model Hamiltonian are determined by classical calculations. The random walk algorithm is employed to find the potential parameters which correspond with the minimum difference between the classical and quantum partial survival probabilities, $\sigma(K,\lambda)=\int \mathrm{d}t\mathrm{d}E|S(t,E;K,\lambda)-Z^{\mathrm{mod}}(t,E)|^2$. ▲ marks the initial guess of the potential parameters, $K=2$ a.u., $\lambda=0.2$ a.u. ■ marks the potential parameters used in the quantum calculation, $K=1$ a.u., $\lambda=0.05$ a.u. The dots mark all the potential parameters for which the difference $\sigma(K,\lambda)$ has been evaluated. The successive points of the "random walker" are connected by a line.

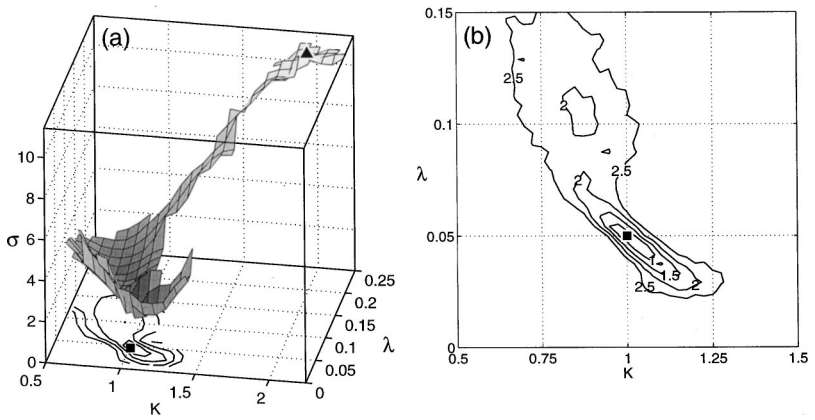

FIG. 11. The difference between the partial survival probabilities $\sigma(K,\lambda)$ as obtained during the optimization calculation. The initial guess of the potential parameters is marked by ▲ and the potential parameters of the benchmark quantum calculation are signed by ■. (a) Shows the incomplete surface obtained from all classical propagations, while (b) represents a zoom around the global minimum.

exceed the uncertainty of the fitted potential, the initial wave function and the transition moments must be parametrized and fitted together with the potential surface. Since classical trajectory calculations scale linearly with the size of the system, the method we propose is supposed to be useful also for large molecules. The applications for real systems are under current study.

VI. CONCLUDING REMARKS

The autocorrelation function is expanded as a linear combination of time dependent terms which are associated with the recurrences. The method we developed enables the identification of the recurrences even when their fingerprints are not observed in the autocorrelation function due to the interference phenomena. This method is based on forward and backward transformations in the time-energy plane which perhaps has a general use in other types of signal from noise analysis.

As an illustrative numerical example we studied the quantum dynamics of a mixed chaotic/regular system. In this case the proposed method enables the identification of the individual recurrences even after many (classical) periods.

The recurrences are very suitable objects for the application of the Wigner phase space method. In spite of the fact that this method is based on classical trajectory calculations only, after a modification it provides the correct amplitudes and phases of the recurrences as obtained from quantum-mechanical calculations. The Wigner phase space method has been widely used before for calculating the amplitudes of the autocorrelation functions. In our modified approach we calculate the partial survival probabilities on different energy shells. We have shown that without doing semiclassical calculations we can evaluate the amplitudes and phases of the recurrences.

Moreover, we have shown that by association a time-independent phase factor to each one of the recurrences the quantum amplitude and phase of the autocorrelation function can be obtained. Therefore, we have obtained the quantum information up to a set of time independent phase factors. It seems very unlikely that these phase factors can be calculated from classical calculations only. However, even without knowing them, just by calculating the amplitudes and phases of the recurrences by using classical mechanics and by comparing them to the results obtained from the analysis of the measured absorption spectra, we can determine the potential energy surface parameters. Under current studies is the use of this method to calculate the molecular potential energy surfaces of three atomic molecular systems.

The modified Wigner phase space method is derived rigorously as a linearization of the semiclassical hydrodynamical moments of the Wigner transform of the recurrences in the autocorrelation function. We show that the Wigner phase space method provides correct results as long as the recurrences do not overlap. The condition under which the modified Wigner phase space method provides correct results and its application to a simple analytically soluble case are under current studies.

ACKNOWLEDGMENTS

This work was supported in part by US-Israel Binational Science Foundation, by the Basic Research Foundation administered by the Israeli Academy of Sciences and Humanities and by the Fund for the Promotion of Research at the Technion. The authors wish to thank Dr. Bilha Segev, Professor Shmuel Fishman, Professor Lorenz S. Cederbaum, and Professor Eric J. Heller for most helpful and enlightening discussions.

APPENDIX:

The underlying idea of the proof is that each one of the recurrences of the classical partial survival probability, $S_m(t,E)$, is formed by a group of close classical trajectories which occupy a small continuous region in phase space. Therefore, trajectories forming $S_m(t,E)$ get the same values of the Maslov index. For the Ehrenfest time of propagation the functions $S_m(t,E)$ appear in disjunct time intervals.

Lemma: Zeroth and first ''hydrodynamical moments'' of the quantum $Z(t,E)$ are evaluated in the semiclassical approximation for the condition that the initial wave packet Ψ occupies a compact small region in the phase space. The zeroth and the first hydrodynamical moments of the quantum $Z_m(t,E)$ can be approximated by the zeroth and the first hydrodynamical moments of $S_m(t,E)$.

Proof: Using the initial value representation of the Van Vleck–Gutzwiller propagator we express the autocorrelation function $C(t)$ [Eq. (1)] in the semiclassical approximation[1,2]

$$C^{\mathrm{SC}}(t)=\int \mathrm{d}\mathbf{q_0}\mathrm{d}\mathbf{p_0}\frac{\sqrt{\det \mathbf{M_{qp}}(\mathbf{q_0},\mathbf{p_0},t)}}{(2\pi i\hbar)^F}\times\exp\left[\frac{i}{\hbar}s(\mathbf{q_0},\mathbf{p_0},t)\right]\Psi(\mathbf{q_t})\Psi^*(\mathbf{q_0}), \tag{A1}$$

where $\mathbf{q_0}$, $\mathbf{p_0}$ are initial position and momentum of a classical trajectory and $\mathbf{q_t}=\mathbf{q}(\mathbf{q_0},\mathbf{p_0},t)$, $\mathbf{p_t}=\mathbf{p}(\mathbf{q_0},\mathbf{p_0},t)$ are final position and momentum. F is the number of degrees of freedom of the studied system. $\mathbf{M_{qp}}$ is one of the Monodromy matrices defined by

$$\mathbf{M_{qq}}(\mathbf{q_0},\mathbf{p_0},t)=\frac{\partial \mathbf{q}(\mathbf{q_0},\mathbf{p_0},t)}{\partial \mathbf{q_0}},\qquad \mathbf{M_{qp}}(\mathbf{q_0},\mathbf{p_0},t)=\frac{\partial \mathbf{q}(\mathbf{q_0},\mathbf{p_0},t)}{\partial \mathbf{p_0}}. \tag{A2}$$

The phase of the semiclassical propagator is given by

$$s(\mathbf{q_0},\mathbf{p_0},t)=\int_0^t \mathrm{d}t'[\mathbf{p}_{\mathbf{t}'}^T\dot{\mathbf{q}}_{\mathbf{t}'}-H(\mathbf{q_0},\mathbf{p_0})]-\frac{\hbar}{2}\pi\nu(\mathbf{q_0},\mathbf{p_0},t). \tag{A3}$$

The Maslov index $\nu(\mathbf{q_0},\mathbf{p_0},t)$ is equal to number of zeros attained by $\det \mathbf{M_{qp}}$ in the time interval $(0,t)$. The semiclassical expression for the autocorrelation function [Eq. (A1)] is substituted into the definitions of the hydrodynamical moments [Eq. (16)]

$$Z_{\mathrm{SC}}^{(n)}(t)=\frac{(-i\hbar)^n}{(2\pi\hbar)^{2F}}\left[\frac{\partial^n}{\partial\tau^n}\int \mathrm{d}\mathbf{q_0'}\mathrm{d}\mathbf{p_0'}\mathrm{d}\mathbf{q_0''}\mathrm{d}\mathbf{p_0''}\times\sqrt{\det \mathbf{M_{qp}}\left(\mathbf{q_0'},\mathbf{p_0'},t-\frac{\tau}{2}\right)\det \mathbf{M_{qp}}\left(\mathbf{q_0''},\mathbf{p_0''},t+\frac{\tau}{2}\right)}\times\exp\left\{\frac{i}{\hbar}\left[s\left(\mathbf{q_0'},\mathbf{p_0'},t-\frac{\tau}{2}\right)-s\left(\mathbf{q_0''},\mathbf{p_0''},t+\frac{\tau}{2}\right)\right]\right\}\times\Psi(\mathbf{q}'_{\mathbf{t}-\tau/2})\Psi^*(\mathbf{q_0'})\Psi^*(\mathbf{q}''_{\mathbf{t}+\tau/2})\Psi(\mathbf{q_0''})\right]_{\tau=0} \tag{A4}$$

The integral in Eq. (A4) comprises correlations between all pairs of classical points, differing in their initial positions, initial momenta, and times. The following change of integration variables introduces the difference between the initial positions and initial momenta $(\Delta\mathbf{q_0},\Delta\mathbf{p_0})$ and the mean initial position and momentum $(\mathbf{q_0},\mathbf{p_0})$

$$\mathbf{q_0'}=\mathbf{q_0}-\frac{\Delta\mathbf{q_0}}{2},\quad \mathbf{q_0''}=\mathbf{q_0}+\frac{\Delta\mathbf{q_0}}{2},\quad \mathbf{p_0'}=\mathbf{p_0}-\frac{\Delta\mathbf{p_0}}{2},\quad \mathbf{p_0''}=\mathbf{p_0}+\frac{\Delta\mathbf{p_0}}{2}. \tag{A5}$$

All functions appearing in the integral Eq. (A4) can be expanded by means of Taylor series by $\Delta\mathbf{q_0}$, $\Delta\mathbf{p_0}$, and τ. Following the approach of Sun, Wang, and Miller[18] we study the first-order term of this expansion in $\Delta\mathbf{q_0}$ and $\Delta\mathbf{p_0}$. The first-order (linear) approximation in the initial positions and momenta is justified for the case where the initial wave packet Ψ occupies a small compact region in phase space. Note that in the work of Sun, Wang, and Miller the correlation in time (introduced in our calculations by carrying out the derivative over τ) has not been studied. Obviously, the first-order expansion in τ is sufficient to obtain correctly only $Z_{\mathrm{SC}}^{(0)}(t)$ and $Z_{\mathrm{SC}}^{(1)}(t)$. The coordinates $\mathbf{q}'_{\mathbf{t}-\tau/2}$ and $\mathbf{q}''_{\mathbf{t}+\tau/2}$ which appear in the arguments of the initial wave packet Ψ in the Eq. (A4) are expressed by the first-order expansion in the distance between the two coupled trajectories $\Delta\mathbf{q_0}$, $\Delta\mathbf{p_0}$, and τ:

$$\mathbf{q}\left(\mathbf{q_0'},\mathbf{p_0'},t-\frac{\tau}{2}\right)=\mathbf{q}(\mathbf{q_0},\mathbf{p_0},t)-\frac{\partial\mathbf{q}}{\partial\mathbf{q_0}}(\mathbf{q_0},\mathbf{p_0},t)\frac{\Delta\mathbf{q_0}}{2}-\frac{\partial\mathbf{q}}{\partial\mathbf{p_0}}(\mathbf{q_0},\mathbf{p_0},t)\frac{\Delta\mathbf{p_0}}{2}-\frac{\partial\mathbf{q}}{\partial t}(\mathbf{q_0},\mathbf{p_0},t)\frac{\tau}{2}, \tag{A6}$$

$$\mathbf{q}\left(\mathbf{q_0''},\mathbf{p_0''},t+\frac{\tau}{2}\right)=\mathbf{q}(\mathbf{q_0},\mathbf{p_0},t)+\frac{\partial\mathbf{q}}{\partial\mathbf{q_0}}(\mathbf{q_0},\mathbf{p_0},t)\frac{\Delta\mathbf{q_0}}{2}+\frac{\partial\mathbf{q}}{\partial\mathbf{p_0}}(\mathbf{q_0},\mathbf{p_0},t)\frac{\Delta\mathbf{p_0}}{2}+\frac{\partial\mathbf{q}}{\partial t}(\mathbf{q_0},\mathbf{p_0},t)\frac{\tau}{2}. \tag{A7}$$

The integral terms in the classical phases $s(\mathbf{q_0'},\mathbf{p_0'},t-\tau/2)$ and $s(\mathbf{q_0''},\mathbf{p_0''},t+\tau/2)$ are expanded by up to the second order of $\Delta\mathbf{q_0}$, $\Delta\mathbf{p_0}$, and τ in the Taylor series expansion. By virtue of symmetry, zeroth- and second-order terms of the expansions are canceled out of the propagator phase

$$s\left(\mathbf{q_0'},\mathbf{p_0'},t-\frac{\tau}{2}\right)-s\left(\mathbf{q_0''},\mathbf{p_0''},t+\frac{\tau}{2}\right)=-\frac{\partial s}{\partial\mathbf{q_0}}(\mathbf{q_0},\mathbf{p_0},t)\Delta\mathbf{q_0}-\frac{\partial s}{\partial\mathbf{p_0}}(\mathbf{q_0},\mathbf{p_0},t)\Delta\mathbf{p_0}-\frac{\partial s}{\partial t}(\mathbf{q_0},\mathbf{p_0},t)\tau-\frac{\hbar}{2}\pi\Delta\nu. \tag{A8}$$

The difference between the Maslov indices of the two contributing trajectories is denoted by $\Delta\nu$. The value of $\Delta\nu$ depends on the initial positions and initial momenta of both involved trajectories and on the classical propagation times. In order to simplify the notation from now we skip on the list of arguments of $\Delta\nu$. The first derivatives of the classical phase $s(\mathbf{q_0},\mathbf{p_0},t)$ are equal to

$$\frac{\partial s}{\partial\mathbf{q_0}}(\mathbf{q_0},\mathbf{p_0},t)=\mathbf{p}_\mathbf{t}^T\mathbf{M_{qq}}(\mathbf{q_0},\mathbf{p_0},t)-\mathbf{p_0}^T,\quad \frac{\partial s}{\partial\mathbf{p_0}}(\mathbf{q_0},\mathbf{p_0},t)=\mathbf{p}_\mathbf{t}^T\mathbf{M_{qp}}(\mathbf{q_0},\mathbf{p_0},t),\quad \frac{\partial s}{\partial t}(\mathbf{q_0},\mathbf{p_0},t)=\mathbf{p}_\mathbf{t}^T\dot{\mathbf{q}}_\mathbf{t}-H(\mathbf{q_0},\mathbf{p_0}). \tag{A9}$$

Consistent with the linear approximation of the trajectories $\mathbf{q}'_{\mathbf{t}-\tau/2}$ and $\mathbf{q}''_{\mathbf{t}+\tau/2}$, the Monodromy matrices [Eq. (A2)] are thus independent of $\Delta\mathbf{q_0}$, $\Delta\mathbf{p_0}$, and τ

$$\mathbf{M_{qp}}\left(\mathbf{q_0'},\mathbf{p_0'},t-\frac{\tau}{2}\right)=\mathbf{M_{qp}}(\mathbf{q_0},\mathbf{p_0},t),\qquad \mathbf{M_{qp}}\left(\mathbf{q_0''},\mathbf{p_0''},t+\frac{\tau}{2}\right)=\mathbf{M_{qp}}(\mathbf{q_0},\mathbf{p_0},t). \tag{A10}$$

The linearized semiclassical approximation to the zeroth and first hydrodynamical moments of the Wigner transform of the autocorrelation function reads

$$Z_{\mathrm{LSC}}^{(n)}(t)=\frac{(-i\hbar)^n}{(2\pi\hbar)^{2F}}\left[\frac{\partial^n}{\partial\tau^n}\int \mathrm{d}\mathbf{q_0}\mathrm{d}\mathbf{p_0}\mathrm{d}\Delta\mathbf{q_0}\mathrm{d}\Delta\mathbf{p_0}\det\mathbf{M_{qp}}(\mathbf{q_0},\mathbf{p_0},t)\exp\left(\frac{i}{2}\pi\Delta\nu\right)\right.$$
$$\times\exp\left\{-\frac{i}{\hbar}([\mathbf{p_t}^T\mathbf{M_{qq}}(\mathbf{q_0},\mathbf{p_0},t)-\mathbf{p_0}^T]\Delta\mathbf{q_0}+\mathbf{p_t}^T\mathbf{M_{qp}}(\mathbf{q_0},\mathbf{p_0},t)\Delta\mathbf{p_0})\right\}\exp\left\{-\frac{i}{\hbar}([\mathbf{p_t}^T\dot{\mathbf{q}}_\mathbf{t}-H(\mathbf{q_0},\mathbf{p_0})]\tau)\right\}\Psi\left(\mathbf{q_0}+\frac{\Delta\mathbf{q_0}}{2}\right)$$
$$\left.\times\Psi^*\left(\mathbf{q_0}-\frac{\Delta\mathbf{q_0}}{2}\right)\Psi\left(\mathbf{q_t}-\mathbf{M_{qq}}\frac{\Delta\mathbf{q_0}}{2}-\mathbf{M_{qp}}\frac{\Delta\mathbf{p_0}}{2}-\dot{\mathbf{q}}_\mathbf{t}\frac{\tau}{2}\right)\Psi^*\left(\mathbf{q_t}+\mathbf{M_{qq}}\frac{\Delta\mathbf{q_0}}{2}+\mathbf{M_{qp}}\frac{\Delta\mathbf{p_0}}{2}+\dot{\mathbf{q}}_\mathbf{t}\frac{\tau}{2}\right)\right]_{\tau=0}. \quad (A11)$$

In order to simplify the arguments of the functions which appear in Eq. (A11), we change the integration variable $\Delta\mathbf{p_0}$ for $\Delta\mathbf{q_t}$ defined by

$$\Delta\mathbf{q_t}=\mathbf{M_{qq}}\Delta\mathbf{q_0}+\mathbf{M_{qp}}\Delta\mathbf{p_0}+\dot{\mathbf{q}}_\mathbf{t}\tau, \quad (A12)$$

$$Z_{\mathrm{LSC}}^{(n)}(t)=\frac{(-i\hbar)^n}{(2\pi\hbar)^{2F}}\left[\frac{\partial^n}{\partial\tau^n}\int \mathrm{d}\mathbf{q_0}\mathrm{d}\mathbf{p_0}\int \mathrm{d}\Delta\mathbf{q_0}\Psi\left(\mathbf{q_0}+\frac{\Delta\mathbf{q_0}}{2}\right)\Psi^*\left(\mathbf{q_0}-\frac{\Delta\mathbf{q_0}}{2}\right)e^{i\mathbf{p_0}^T\Delta\mathbf{q_0}/\hbar}\int \mathrm{d}\Delta\mathbf{q_t}\Psi\left(\mathbf{q_t}-\frac{\Delta\mathbf{q_t}}{2}\right)\right.$$
$$\left.\times\Psi^*\left(\mathbf{q_t}+\frac{\Delta\mathbf{q_t}}{2}\right)e^{-i\mathbf{p_t}^T\Delta\mathbf{q_t}/\hbar}\exp\left\{\frac{i}{\hbar}H(\mathbf{q_0},\mathbf{p_0})\tau\right\}e^{i\pi\Delta\nu/2}\right]_{\tau=0}. \quad (A13)$$

By taking the τ derivatives Eq. (A13) is reduced to

$$Z_{\mathrm{LSC}}^{(n)}(t)=\frac{1}{(2\pi\hbar)^{2F}}\int \mathrm{d}\mathbf{q_0}\mathrm{d}\mathbf{p_0}\int \mathrm{d}\Delta\mathbf{q_0}\Psi\left(\mathbf{q_0}+\frac{\Delta\mathbf{q_0}}{2}\right)\Psi^*\left(\mathbf{q_0}-\frac{\Delta\mathbf{q_0}}{2}\right)e^{i\mathbf{p_0}^T\Delta\mathbf{q_0}/\hbar}\int \mathrm{d}\Delta\mathbf{q_t}\Psi\left(\mathbf{q_t}-\frac{\Delta\mathbf{q_t}}{2}\right)$$
$$\times\Psi^*\left(\mathbf{q_t}+\frac{\Delta\mathbf{q_t}}{2}\right)e^{-i\mathbf{p_t}^T\Delta\mathbf{q_t}/\hbar}[H(\mathbf{q_0},\mathbf{p_0})]^n\exp\left(\frac{i\pi\Delta\nu_{\tau=0}}{2}\right). \quad (A14)$$

For the Ehrenfest propagation time the recurrences on $S(t,E)$ appear in disjunct time intervals. For the given time t within the time interval of the recurrence $S_m(t,E)$, all trajectories acquire the same Maslov index. Therefore, $\Delta\nu=0$ and we obtain from Eq. (A14) the semiclassical approximation for the first and second hydrodynamical moments given by

$$Z_{m,\mathrm{LSC}}^{(n)}(t)=\frac{1}{(2\pi\hbar)^{2F}}\int \mathrm{d}\mathbf{q_0}\mathrm{d}\mathbf{p_0}\int \mathrm{d}\Delta\mathbf{q_0}\Psi\left(\mathbf{q_0}+\frac{\Delta\mathbf{q_0}}{2}\right)\Psi^*\left(\mathbf{q_0}-\frac{\Delta\mathbf{q_0}}{2}\right)e^{i\mathbf{p_0}^T\Delta\mathbf{q_0}/\hbar}\int \mathrm{d}\Delta\mathbf{q_t}\Psi\left(\mathbf{q_t}-\frac{\Delta\mathbf{q_t}}{2}\right)$$
$$\times\Psi^*\left(\mathbf{q_t}+\frac{\Delta\mathbf{q_t}}{2}\right)e^{-i\mathbf{p_t}^T\Delta\mathbf{q_t}/\hbar}[H(\mathbf{q_0},\mathbf{p_0})]^n. \quad (A15)$$

Hence proved

$$Z_{m,\mathrm{LSC}}^{(n)}(t)=S_m^{(n)}(t),\quad n=\{0,1\}. \quad (A16)$$

For the propagation after the lapse of the Ehrenfest time, the trajectories are divided into groups according to the values of their Maslov index. Then, the semiclassical approximation to the autocorrelation function $C^{\mathrm{SC}}(t)$ is a sum over contributions, $C_\nu^{\mathrm{SC}}(t)$, given by

$$C_\nu^{\mathrm{SC}}(t)=\int_\nu \mathrm{d}\mathbf{q_0}\mathrm{d}\mathbf{p_0}\frac{\sqrt{\det\mathbf{M_{qp}}(\mathbf{q_0},\mathbf{p_0},t)}}{(2\pi i\hbar)^F}$$
$$\times\exp\left[-\frac{i}{\hbar}s(\mathbf{q_0},\mathbf{p_0},t)\right]\Psi^*(\mathbf{q_t})\Psi(\mathbf{q_0}). \quad (A17)$$

The linear approximation of the zeroth and first hydrodynamical moments of the component $C_\nu^{\mathrm{SC}}(t)$ leads to

$$Z_{\nu,\mathrm{LSC}}^{(n)}(t)=S_m^{(n)}(t),\quad n=\{0,1\}. \quad (A18)$$

Since from the zeroth and first hydrodynamical moments of $Z(t,E)$ one can calculate the time-dependent amplitude and phase of the recurrences of the autocorrelation function $C_m(t)$ (up to time-independent phase factor), it is clear that on the basis of Eq. (A18) one can evaluate $C_m(t)$ from classical trajectory calculations only.

[1] J. H. Van Vleck, Proc. Natl. Acad. Sci. U.S.A. **14**, 178 (1928); M. C. Gutzwiller, J. Math. Phys. **8**, 1979 (1967).
[2] W. H. Miller, J. Chem. Phys. **53**, 3578 (1970).
[3] E. J. Heller, J. Chem. Phys. **94**, 2723 (1991).
[4] M. F. Herman and E. Kluk, Chem. Phys. **91**, 27 (1984); E. Kluk, M. F. Herman, and H. L. Davis, J. Chem. Phys. **84**, 326 (1986); M. F. Herman, *ibid.* **85**, 2069 (1986).
[5] K. G. Kay, J. Chem. Phys. **100**, 4377 (1994); **100**, 4432 (1994).
[6] B. W. Spath and W. H. Miller, Chem. Phys. Lett. **262**, 486 (1996); X. Sun and W. H. Miller, J. Chem. Phys. **106**, 916 (1997).
[7] M. A. Sepulveda and E. J. Heller, J. Chem. Phys. **101**, 8004 (1994); **101**, 8016 (1994).
[8] A. R. Walton and D. E. Manopoulos, Mol. Phys. **87**, 961 (1996); A. R. Walton and D. E. Manopoulos, Chem. Phys. Lett. **224**, 448 (1995); M. L. Brewer, J. S. Hulme, and D. E. Manopoulos, J. Chem. Phys. **106**, 4832 (1997).
[9] F. Grossmann, Chem. Phys. Lett. **262**, 470 (1996).
[10] S. Garashchuk and D. Tannor, Chem. Phys. Lett. **262**, 477 (1996).
[11] J. L. Schoendorff, H. J. Korsch, and N. Moiseyev, Europhys. Lett. **44**, 290 (1998).
[12] M. A. Sepulveda and F. Grossmann, Adv. Chem. Phys. **XCVI**, 191 (1996).
[13] M. Ovchinnikov and V. A. Apkarian, J. Chem. Phys. **105**, 10312 (1996); **108**, 2277 (1998).

[14] E. J. Heller, J. Chem. Phys. **75**, 2923 (1981); **62**, 1544 (1975).
[15] E. J. Heller, J. Chem. Phys. **65**, 1289 (1976); **75**, 186 (1981).
[16] E. Wigner, Phys. Rev. **40**, 749 (1932); J. E. Moyal, Proc. Cambridge Philos. Soc. **45**, 99 (1949); K. Imre, E. Ozizmir, and P. F. Zweifel, J. Math. Phys. **8**, 1097 (1967); M. Hillery, R. F. O'Connell, M. O. Scully, and E. P. Wigner, Phys. Rep. **106**, 121 (1984); H-W. Lee, *ibid.* **259**, 147 (1995).
[17] S. Garashchuk and D. Tannor, Chem. Phys. Lett. **263**, 324 (1996).
[18] X. Sun, H. Wang, and W. H. Miller, J. Chem. Phys. **109**, 7064 (1998); **109**, 4190 (1998); **108**, 9726 (1998); X. Sun, *ibid.* **112**, 8241 (2000).
[19] R. A. Pullen and A. R. Edmonds, J. Phys. A **14**, L477 (1981); E. Haller, H. Koppel, and L. S. Cederbaum, Phys. Rev. Lett. **52**, 1665 (1984).
[20] M. Feingold, N. Moiseyev, and A. Peres, Chem. Phys. Lett. **117**, 344 (1985); N. Moiseyev, R. C. Brown, R. E. Wyatt, and E. Tzidoni, *ibid.* **127**, 37 (1986); N. Moiseyev, R. Friesner, and R. E. Wyatt, J. Chem. Phys. **85**, 331 (1986).
[21] N. Moiseyev and A. Peres, J. Chem. Phys. **79**, 5945 (1983); M. Feingold, N. Moiseyev, and A. Peres, Phys. Rev. A **30**, 509 (1984); N. Moiseyev, *Lecture Notes in Physics*, (Springer, New York, 1985), Vol. 256, pp. 122–131.
[22] P. Zdanska, L. S. Cederbaum, and N. Moiseyev (*in preparation*).
[23] T. P. Wang, A. H. Wagnucci, and C. C. Li, *Digital Signal Processing—91, Proceedings of the International Conference* (Elsevier, Amsterdam, Netherlands; 1991); xvii+765, p. 91; S. Qian and J. M. Moris, Signal Process. **27**, 125 (1992); I. Cohen, S. Raz, and D. Malah, *ibid.* **73**, 203 (1999).
[24] R. Schinke, *Photodissociation Dynamics* (Cambridge University Press, Cambridge, 1993).